SIMULATION RESEARCH ON HEAT RECOVERY SYSTEM OF HEAT PUMP COMPOSITE PUMP-DRIVEN LOOP HEAT PIPE

by

Shuailing LIU, Guoyuan MA, Xiaoya JIA, Shuxue XU[*], and Guoqiang WU

Department of Refrigeration and Cryogenic Engineering, Beijing University of Technology, Beijing, China

To promote energy-saving potentials of the energy recovery unit under all-year conditions, a composite system combining pump-driven loop heat pipe with heat pump was firstly proposed, and the mathematical models were established. The operating characteristics of the composite system were studied in the whole year and compared with the traditional heat pump heat recovery system. The results show that the heating capacity of the composite system is in line with the heating load in winter. Compared with the traditional heat pump system, the composite system has higher energy efficiency ratio and lower deviation degree of temperature effectiveness in the whole year. The heat pump composite pump-driven loop heat pipe heat recovery system is generally superior to similar system reported in literatures, which indicates that it can replace heat pump system in buildings ventilation.

Keywords*: heat pump, heat-pipe, heat recovery, composite,*
energy-saving, simulation

Introduction

Nowadays, energy conservation and emission reduction has gradually become the mainstream trend [1]. According to statistics, building sector accounts for 30-40% of the global final energy consumption and 30% of total CO_2 emissions [2]. To reduce buildings energy consumption, high-performance buildings such as passive house and ultra-low energy building has been researched, developed, and promoted [3]. Ultra-low energy buildings mainly reduce energy demand by improving heat insulation effectiveness and the air-tightness. However, it will lead to the risk of sick building syndrome in ultra-low energy buildings without fresh air system [4, 5]. The mechanical ventilation system can solve the aforementioned problems, but it will cause a great loss of energy sources [6]. A mechanical ventilation with heat recovery system is wildly used to solve this issue, which can significantly reduce the buildings energy consumption [7]. Li *et al.* [8] revealed that when the sensible effectiveness of the heat recovery units reached 70%, half of the building heating consumption could be reduced.

At present, air-to-air heat recovery units such as fixed plate, plate-fin, energy wheel, heat pipe, run-around, and heat pump (HP), are commonly used in buildings ven-

_____
[*]Corresponding author, e-mail: xsx@bjut.edu.cn

4302

Liu, S., *et al.*: Simulation Research on Heat Recovery System of …
THERMAL SCIENCE: Year 2022, Vol. 26, No. 5B, pp. 4301-4313

tilation [9-11]. Fixed plate, plate-fin and energy wheel heat recovery units have higher heat recovery efficiency, but installation space must be required. Moreover, when the heat exchanger is adopted in cold climates, the ice and frost are often observed inside exchanger channels which usually degrade the exchanger performance [12]. Run-around heat recovery unit uses water with antifreeze as working fluid in winter, and the temperature effectiveness of the unit is usually 45-55% [13]. The heat pipe heat recovery unit has been commonly used in naturally ventilated buildings due to its advantages, such as easy manufacturing, no moving parts, no cross contamination and so on. The temperature effectiveness is about 50%. However, it is hard to meet the requirements of the large-scale ventilation system [14]. The HP heat recovery system belongs to active heat recovery unit. When the temperature difference between indoor and outdoor is smaller enough, the temperature efficiency will reach 100% [15].

Pump-driven loop heat pipe (PLHP) and HP heat recovery units has been widely used to recover the heat in buildings ventilation. Ma *et al.* [16] experimentally studied the working characteristics and influencing parameters of the PLHP heat recovery unit, and the temperature effectiveness of the system was only 30-40% in winter. Zhu *et al.* [17] proposed a pump-driven multi-loop heat pipe heat recovery system to promote the temperature effectiveness by improving the uniformity of the heat transfer temperature difference. Zhou *et al.* [18] compared and analyzed the thermal performance of single-loop and multi-loop PLHP heat recovery units. The results showed that compared with the single-loop unit, the temperature effectiveness of the multi-loop unit was improved slightly. Chen [19] found that HP heat recovery system had high energy-saving potential. Wang [20] carried out an experimental study of traditional HP heat recovery system. When the outdoor temperature (OT) dropped from 15 ℃ to –15℃, the temperature effectiveness decreased from 319.25% to 62%, while the energy efficiency ratio (EER) increased from 3.4 to 6.9. Cao *et al*. [21] proposed a stepped pressure cycle instead of the vapor-compression cycle to improve the energy efficiency. Jia *et al*. [22] studied the thermal performance of the dual-loop HP heat recovery system. The results showed that when OT was below 0 ℃ in winter conditions, the heating capacity and EER would be greatly reduced.

From the aforementioned literature review, PLHP, as a passive heat recovery device, exists a limited value of temperature effectiveness [23]. However, this system has a higher heat transfer capacity and EER under a great temperature difference between indoor and outdoor. In other words, this system cannot handle the all-year fresh air load alone [24]. The HP heat recovery system belongs to active heat recovery device existing a much higher temperature effectiveness, even exceeding 100%. However, the energy efficiency of the system is lower [15]. Lots of literature have studied the thermal performance of the PLHP and HP heat recovery system, respectively. However, a composite system combining the PLHP with HP has few literatures studied in buildings ventilation.

In this paper, to exploit the advantages of the PLHP and the HP heat recovery system, a composite system combining HP with pump-driven loop heat pipe (HPCP) is proposed. The novel integrated unit can recover part of exhaust air energy by PLHP system, then recover most of the exhaust air energy by HP system. The energy of the exhaust air can be recycled step by step. A mathematical model of HPCP is established, and R32 is selected as working fluid. Based on the model, a steady-state simulation of the HPCP is carried out by using MATLAB and REFPROP. The effect of the temperature difference between indoor and outdoor on the fresh air outlet temperature, input power, heat transfer capacity, temperature effectiveness and EER are researched and compared with traditional HP system.

Working principle and components model

Working principle

Figures 1 and 2 are schematic diagrams of HP and HPCP system, respectively. The HP system is mainly composed of compressor, exhaust air heat exchanger, fresh air heat exchanger, gas-liquid separator, expansion valve, four-way reversing valve, and two centrifugal fans. The HPCP system is mainly consisted of compressor, pump, exhaust air exchanger, fresh air exchanger, gas-liquid separator, reservoir, expansion valve, four-way reversing valve, 1-4 four cut-off valves, and two centrifugal fans.
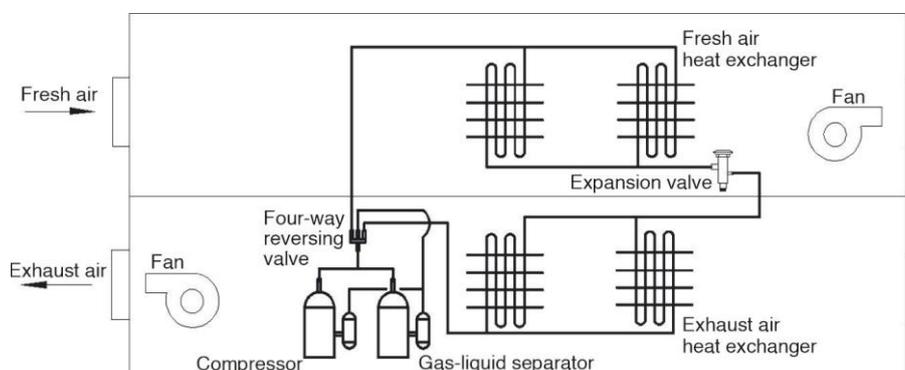
Figure 1. Principle diagram of HP heat recovery system
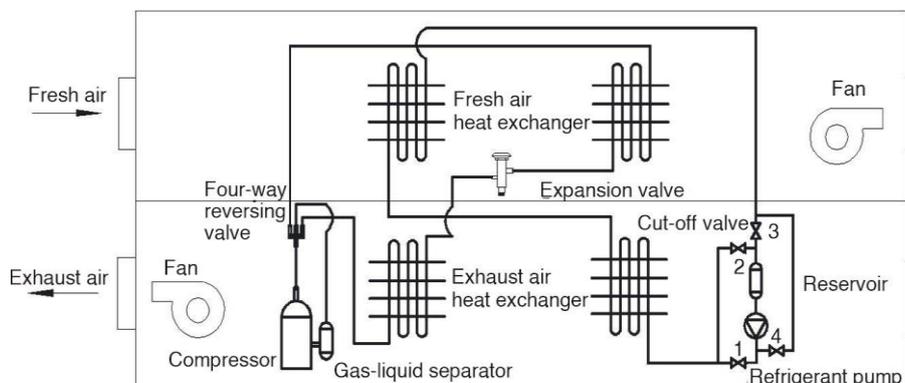
Figure. 2 Principle diagram of HP composite PLHP heat recovery system

Using the four-way directional valve and cut-off valve to achieve the conversion between winter and summer conditions. In HP system, four-way directional valve can be used to change the flow direction of working fluid. In PLHP system, No. 1 and 3 valves are open, and No. 2 and 4 valves are close for the winter conditions. On the contrary, in summer conditions, No. 2 and 4 valves are open, and No. 1 and 3 valves are closed.

For HP system, the working fluid absorbs the energy from the exhaust air in the evaporator and is in the superheated gaseous state. Then the fluid is sucked into the compressor to lift its pressure, and becomes sub-cooled liquid state after discharging energy to the fresh air in the condenser. Finally, the working fluid flows back to the evaporator at low temperature and low pressure state after passing through the expansion valve, and then enters the next cycle.

4304

Liu, S., *et al.*: Simulation Research on Heat Recovery System of …
THERMAL SCIENCE: Year 2022, Vol. 26, No. 5B, pp. 4301-4313

For HPCP system, the fresh air and exhaust air exchange heat in the PLHP system, and part of exhaust air energy is released into the fresh air. Then, heat of the fresh air and exhaust air is exchanged in the HP system. Finally, the fresh air is supplied indoors and the exhaust air is discharged outdoors.

Components modeling

To simplify the calculation process, some assumptions are:
−   The suction superheat of the compressor is 7 ℃ and the inlet subcooling of pump is 5 ℃.
−   The pump and compressor operate at a constant speed. It is assumed that the isentropic efficiency of the compressor is 0.9, the compression process of pump is isothermal, and the throttling process of expander valve is isenthalpic.
−   Homogeneous model is adopted in heat transfer process.

Condenser

Dittus-Boeler formula is adopted for single-phase condensation heat transfer of refrigerant in tube, and Shah formula is used for two-phase [25]:

$$\text{Nu} = \frac{\alpha_{\text{tp}} D}{\lambda_l} = \text{Nu}_l \left[\left(1-x\right)^{0.8} + \frac{3.8 x^{0.76} \left(1-x\right)^{0.04}}{\text{Pr}^{0.38}} \right] \tag{1}$$

$$\text{Pr} = \frac{p}{p_c} \tag{2}$$

$$\text{Nu}_l = \frac{\alpha_l D}{\lambda_l} = 0.023 \left(\frac{GD}{\mu_l} \right)^{0.8} \text{Pr}_l^{0.4} \tag{3}$$

where Nu is the Nusselt number, α_{tp} [Wm^{-2}K^{-1}] – the two-phase heat transfer coefficient, D [mm,] – the outer tube diameter, λ_l [Wm^{-1}K^{-1}] – the liquid phase thermal conductivity, x – the mass gas content rate (Dryness fraction), Pr – the Prandtl number, p [Pa] – the condensation pressure, p_c [Pa] – the critical pressure, G [kgm^{-2}s^{-1}] – the refrigerant mass flow-rate, and μ_l [Pa·s] – the liquid phase viscosity.

Single-phase pressure drop on refrigerant-side of the heat transfer process is not significant. Therefore, it is not considered in the thermodynamic model. For two-phase flow section, only the frictional pressure drop is considered, and its calculation formula is eqs. (4)-(11) [26]:

$$\Delta p_{\text{f}} = \left(E + \frac{3.24 FH}{\text{Fr}^{0.45} \text{We}^{0.035}} \right) \Delta p_l \tag{4}$$

$$\Delta p_l = f_l \frac{L}{D} \frac{G^2}{2\rho_l} \tag{5}$$

$$E = \left(1-x\right)^2 + x^2 \left(\frac{\rho_l f_{\text{g}}}{\rho_{\text{g}} f_l} \right) \tag{6}$$

$$F = x^{0.78} \left(1-x\right)^{0.224} \tag{7}$$

Liu, S., *et al.*: Simulation Research on Heat Recovery System of ...
THERMAL SCIENCE: Year 2022, Vol. 26, No. 5B, pp. 4301-4313

4305

$$H = \left(\frac{\rho_l}{\rho_g}\right)^{0.91} \left(\frac{\mu_g}{\mu_l}\right)^{0.19} \left(1 - \frac{\mu_g}{\mu_l}\right)^{0.7} \tag{8}$$

$$\mathrm{Fr} = \frac{G^2}{gD\rho_{tp}^2} \tag{9}$$

$$\mathrm{We} = \frac{G^2 D}{\sigma \rho_{tp}} \tag{10}$$

$$\rho_{tp} = \left(\frac{x}{\rho_g} + \frac{1-x}{\rho_l}\right)^{-1} \tag{11}$$

where f_l is the liquid-phase friction coefficient, L [m] – the tube length, ρ_l [kgm^{-3}] – the liquid-phase flow density, f_g – the gas-phase friction coefficient, μ_g [Pa·s] – the gas-phase viscosity, σ [Nm^{-1}] – the surface tension, and ρ_{tp} [kgm^{-3}] – the homogeneous flow density.

Evaporator

If the wall temperature of the heat exchangers is lower than the dewpoint temperature, condensation will generate. The dehumidification coefficient is:

$$\xi = \frac{h - h_b}{c_p(t - t_b)} \tag{12}$$

where ξ is the dehumidification coefficient, h [kJkg^{-1}] – the inlet enthalpy of moist air, h_b [kJkg^{-1}] – the enthalpy of saturated air at the surface of a water film, c_p [Jkg^{-1}K^{-1}] – the specific heat capacity of moist air, t [ºC] – the inlet temperature of moist air, and t_b [ºC] – the temperature of saturated air at the surface of a water film.

The boiling heat transfer coefficient in refrigerant tube is calculated by the Gungor-winterton correlation formula [27]:

$$h_{tp} = SS_2 h_{nb} + FF_2 h_{sp} \tag{13}$$

$$h_{nb} = 0.00122 \left(\frac{\lambda_l^{0.79} c_{p,l}^{0.45} \rho_l^{0.49}}{\sigma^{0.5} \mu_l^{0.29} q_r^{0.24} \rho_g^{0.24}}\right) \Delta T_{sat}^{0.24} \Delta p_{sat}^{0.75} \tag{14}$$

$$S = \frac{1}{1 + 1.15 \cdot 10^{-6} F^2 \mathrm{Re}_l^{1.17}} \tag{15}$$

$$F = 1 + 2.4 \cdot 10^4 \mathrm{Bo}^{1.16} + 1.37 \left(\frac{1}{X_{tt}}\right) \tag{16}$$

$$S_2 = \begin{cases} \mathrm{Fr}_l^{0.5} & \text{Horizontal and } \mathrm{Fr}_l < 0.05 \\ 1 & \text{Others} \end{cases} \tag{17}$$

$$F_2 = \begin{cases} \mathrm{Fr}_l^{(0.1-2\mathrm{Fr}_l)} & \text{Horizontal and } \mathrm{Fr}_l < 0.05 \\ 1 & \text{Others} \end{cases} \tag{18}$$

4306

Liu, S., *et al.*: Simulation Research on Heat Recovery System of …
THERMAL SCIENCE: Year 2022, Vol. 26, No. 5B, pp. 4301-4313

where h_{tp} [$\mathrm{Wm^{-2}K^{-1}}$] is the two-phase heat transfer coefficient, q_r [$\mathrm{kJkg^{-1}}$] – the latent heat of refrigerant, ΔT_{sat} [ºC]– the excess temperature, Δp_{sat} [Pa] – the excess pressure, Re_l – the Reynolds number, Bo – the boiling feature number, Fr_l – the Froude number, and X_{tt} – the Lockhart-Martinelli number.

The pressure drop calculation formulas of evaporator are the same as that of condenser.

Major parameters

Calculation conditions

The calculation is performed to comply with the National Standard of the People´s Republic of China GB/T 7725-2016 Room air conditioning [28]. The test conditions are shown in tab. 1.

Table 1. Test operating conditions

Condition	Indoor temperature [ºC]	Indoor relative humidity [%]	OT [ºC]
Winter	20	30%	15, 10, 5, 0, –5, –10, –15
Summer	27	50%	30, 32, 34, 36, 38, 40

Heat exchanger structure

Both fresh air and exhaust air heat exchangers adopt the fin-tube heat exchangers, and the area and the face velocity of heat exchanger are 18 $\mathrm{m^2}$ and 2.6 m/s, respectively. Table 2 indicates the detail parameters of the heat exchangers.

Table 2. Specifications of the heat exchanger

Parameter	Symbol	Value [mm]	Parameter	Symbol	Value [mm]
Outer tube diameter	d_o	9.52	Number of tube columns	n_y	3
Tube thickness	δ	0.35	Tube space	s_x	25.4
Inner tube diameter	d_i	8.82	Tube row space	s_y	22
Tube length	L	900	Fin thickness	δ_f	0.1
Number of tube rows	n_x	18	Fin spacing	s_f	2.12

Selection of compressor and pump

Based on the calculation results of heat transfer capacity and flow resistance, the parameters of the compressor and pump are: The frequency of the power for the compressor with displacement of 36 $\mathrm{cm^3}$ is 50 Hz. Hence, the speed of the compressor is 2880 rpm. The pump nominal input power is 0.35 kW, the maximum pumping head is 25 m, the flow volume rate is 20 Lpm, and the motor speed is 2800 rpm.

Performance evaluation

The performance of the HP and HPCP systems are evaluated by heat transfer capacity, Q, input power, P, temperature efficiency, η, EER, and deviation degree, De. The related equations are:
– The heat transfer capacity, Q:

$$Q = \dot{m}\left(h_{21} - h_{22}\right) \tag{19}$$

where $\dot{m}$ [kgs^{-1}] is the air mass-flow rate, h_{21} [kJkg^{-1}] – the inlet enthalpy of fresh air, h_{22} [kJkg^{-1}] – the outlet enthalpy of fresh air.

– Total power input, P:

$$P = P_c + P_p + P_{fan} \tag{20}$$

where P_c, P_p, P_{fan} [kW] are the input power of compressor, pump, and fans, respectively.

– Temperature efficiency, η:

$$\eta = \frac{t_{21} - t_{22}}{t_{21} - t_{11}} \tag{21}$$

where t_{21}, t_{22} [ºC] are the inlet and outlet temperature of fresh air, respectively and t_{11} [ºC] – the inlet temperature of exhaust air.

– The EER:

$$EER = \frac{Q}{P} \tag{22}$$

where Q [kW] is the total heat transfer capacity and P [kW] – the total input power.

– Deviation degree, De:

$$De = \frac{|A - X|}{A} \tag{23}$$

where A is the target data and X – the actual data.

Model validation

Literature [20, 23] experimentally researched on HP system and PLHP system in building ventilation, respectively. The experimental results are used to validate mathematical model. Figures 3 and 4 shows the heat transfer capacity verification results of HP and PLHP system, respectively. It indicates that the simulation results agree with experimental data well, and the error is within about 10%.
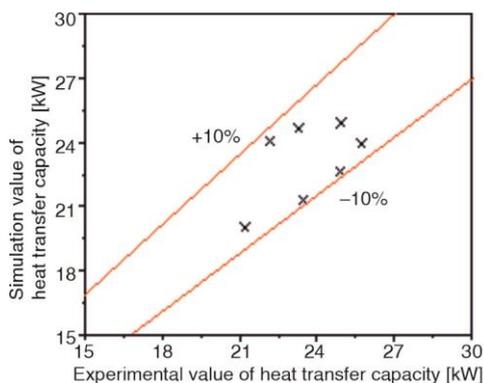
Figure 3. The HP system
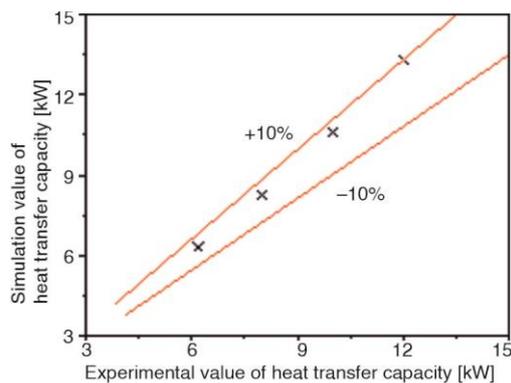
Figure 4. The PLHP system

Results and analysis

Fresh air outlet temperature

Figure 5 shows the fresh air outlet temperature of the HP and HPCP at the different OT. In winter conditions, with the decreases of OT, the outlet temperature of fresh air also decreases gradually. When OT decreases from 15 ºC to –15ºC, the outlet temperature of the

HPCP and HP drops from 25.5 ℃ to 1 ℃ and 32 ℃ to –2 ℃, respectively. With the decreases of OT, the difference of fresh air outlet temperature between HPCP and HP declines gradually. When the OT is –7 ℃, the difference is approximately equal. When the OT increases from 30 ℃ to 40 ℃, the outlet temperature of the HPCP and HP rises from 22 ℃ to 29 ℃ and 18 ℃ to 26.5 ℃, respectively.
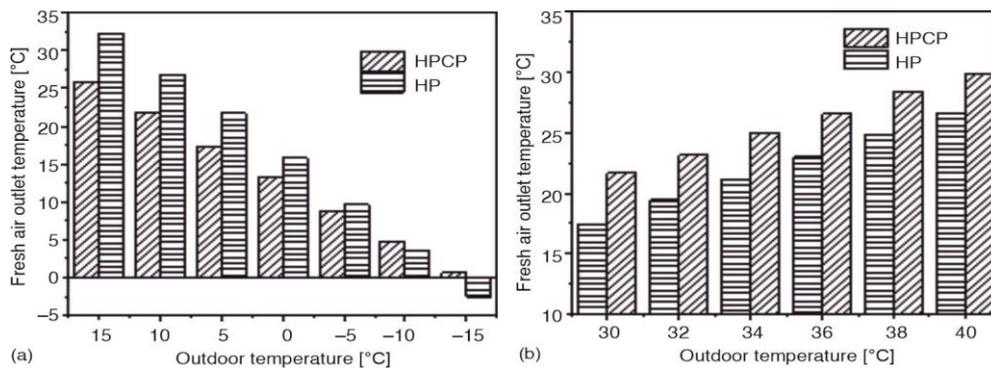
Figure 5. Fresh air outlet temperature; (a) winter conditions and (b) summer conditions

Input power

Figure 6 shows the input power of the system under different conditions. In winter conditions, when the OT decreases from 15 ℃ to –15℃, the input power of HPCP and HP drops from 3.0 kW to 2.2 kW and 5.5 kW to 3.0 kW, respectively. The main reason is that the temperature of the fresh air from the outdoor side is lower, which improves the speed of the refrigerant condensation and reduces the condensation pressure. While the temperature of the exhaust air from the indoor side is constant, the evaporator pressure also decreases, but not significantly. Therefore, with the decreases of OT, the pressure ratio also decreases. As we all know, when the other components have barely changed under different operating conditions, the pressure ratio is the main factor affecting the power consumption of the system. In summer conditions, when the OT increases from 30 ℃ to 40 ℃, the input power of HPCP and HP rises from 3.5 kW to 3.7 kW and 6.5 kW to 6.9 kW, respectively. The main reason why HP has a higher input power than HPCP is that pump is used to overcome the flow resistance of working fluid in pipe. The compressor, however, also needs to compress the gaseous refrigerant other than overcoming the flow resistance of the working fluid.
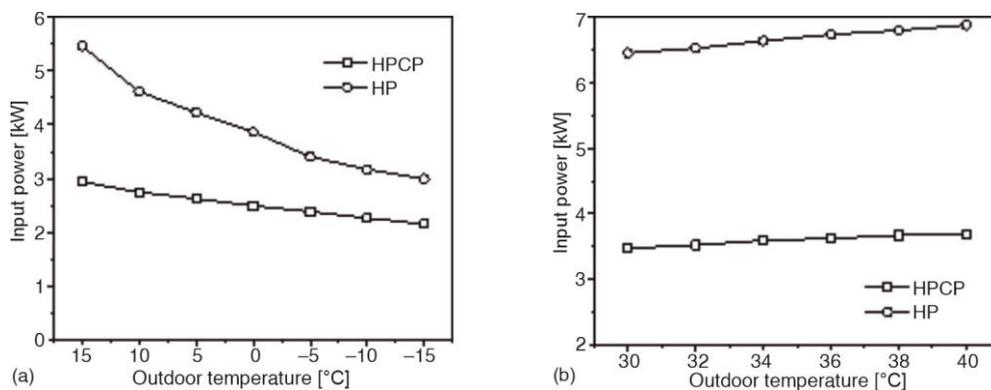
Figure 6. Input power; (a) winter conditions and (b) summer conditions

Heating and cooling capacity

Figure 7 shows the heat transfer capacity of the system under different conditions. Under winter conditions, the heating capacity of HPCP increases gradually, while HP increases at first and then declines with the increases of the OT. The prime reason is that the evaporator pressure and condensation pressure decrease with the OT decreases. Due to the constant temperature of the indoor exhaust air, it increases the heat transfer temperature difference of the evaporator and promotes the recovery rate of waste heat. However, when OT continuously decreases, it is hard for HP system to improve the heating capacity as the mass-flow rate of working fluid decreases sharply due to the increases of saturated gaseous refrigerant specific volume. However, it has less effect on the PLHP system.

When the OT drops from 15 ℃ to –15℃, the heating capacity of the HPCP increases from 15.5 kW to 25 kW, while HP increases first from 24 kW to 25 kW and then reduces to 20 kW. When the OT is –7 ℃, the heating capacity of HPCP and HP is basically equal. Under summer conditions, the cooling capacity of HPCP and HP increases gradually with the increases of evaporation temperature. When the OT increases from 30 ℃ to 40 ℃, the cooling capacity of the HPCP and HP increases from 15 kW to 22 kW and 25 kW to 31 kW, respectively. The cooling capacity of the HP is 40% higher than that of the HPCP, and the extra cooling capacity of the HP system is used to deal with latent heat.
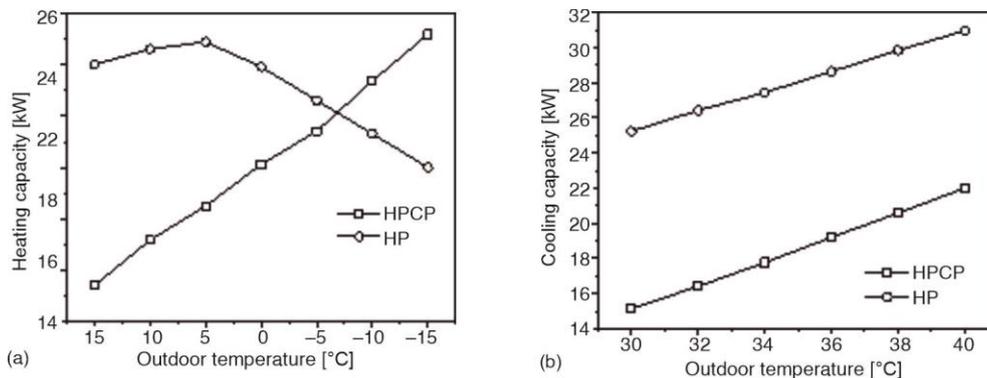
Figure 7. Heat transfer capacity; (a) winter conditions and (b) summer

The EER

The EER is an important parameter for system energy-saving evaluation. The variation of the system EER can be shown in fig. 8. Under winter conditions, with the decreases of OT, the heating EER of HPCP and HP all increases gradually. When the OT drops from 15 ℃ to –15℃, the heating EER of the HPCP and HP increases from 5.2 to 11.5 and 4.5 to 7.8, respectively. When the OT is –15 ℃, the heating EER of HPCP is 50% higher than that of HP system. The EER is the ratio of the heat transfer capacity and input power, which indicates that the EER depends closely on the change of heat transfer capacity and input power. For HP system, in winter conditions, with the decreases of OT, the heating capacity increases firstly and then declines, and the input power decreases. The EER increases with the decreases of the OT because the descent speed of the heating capacity is lower than that of the input power within the range of the calculation temperature. In addition, it can be predicted that the EER will decline with the continuous decreases of OT. For HPCP system, with the decreases of the OT, the heating capacity increases and the input power decreases. So, the change of the EER is

4310

Liu, S., *et al.*: Simulation Research on Heat Recovery System of …
THERMAL SCIENCE: Year 2022, Vol. 26, No. 5B, pp. 4301-4313

the same as that of the heating capacity. Under summer conditions, with the increases of OT, the cooling EER of HPCP and HP also increases gradually. When the OT increases from 30 ℃ to 40 ℃, the cooling EER of the HPCP and HP increases from 4.3 to 6.0 and 3.9 to 4.5, respectively. When the OT is 40 ℃, the cooling EER of HPCP is 35% higher than that of HP system.
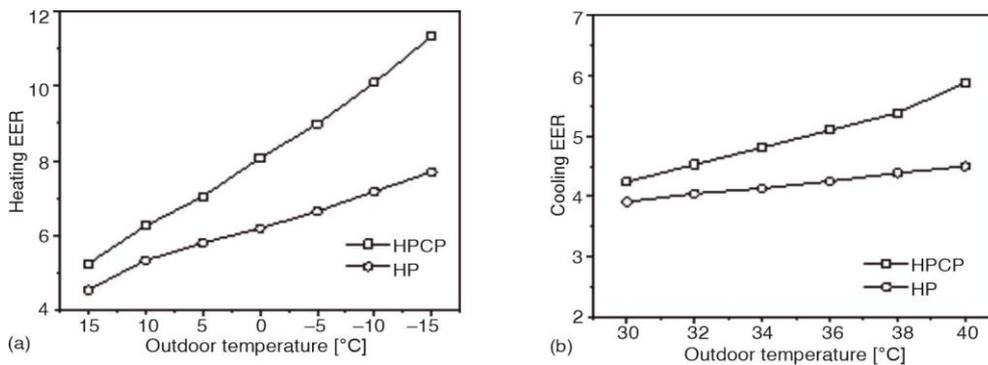
Figure 8. The EER; (a) winter conditions and (b) summer conditions

Temperature effectiveness

Temperature effectiveness reflects the recovery level of the exhaust heat recovery system, which is an important parameter to evaluate the performance of the heat recovery unit. Figure 9 shows the variation of temperature effectiveness under winter and summer conditions. In winter conditions, with decreases of OT, the temperature effectiveness of HPCP and HP falls from 220% to 45% and 345% to 35%, respectively. In summer conditions, with increases of OT, the temperature effectiveness of HPCP and HP falls from 400% to 102% and 275% to 80%, respectively. The red mark is the temperature efficiency value under the standard operating conditions of GB/T 21087-2020 Energy Recovery Ventilators for outdoor Air Handling [29]. As can be seen from fig. 9, the temperature efficiency of HPCP and HP meets the requirements in the whole year.
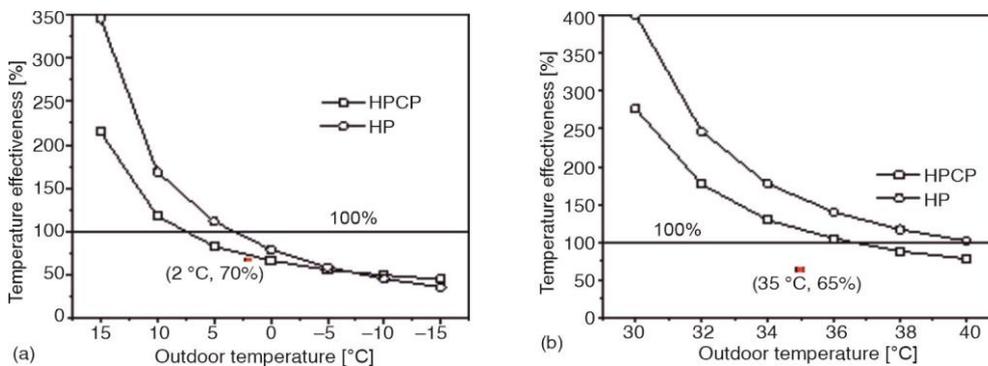
Figure 9. Temperature effectiveness; (a) winter conditions and (b) summer conditions

For the energy recovery in the ventilation system, the load requirements of the fresh air should be met firstly, and the load approaches zero if the temperature effectiveness is close to 100%, while followed by the system performance, such as input power, EER and so on. Deviation is used to evaluate the deviation degree between actual value and target value. The

temperature fluctuation of indoor decreases with the decreases of the deviation degree. Under winter and summer conditions, the deviation degree of HPCP is 3.3 and 3.4, respectively, while that of HP is 5.1 and 5.8. Results show that the temperature effectiveness of HPCP is closer to 100% than that of HP in the whole year.

Comparison with other similar systems

Table 3 shows a comparison of the composite system (HP + PLHP) with the similar systems. Seldom literatures could be found on the application of the HP composite fixed-plate or HP composite energy wheel systems in cold climates. It may be due to the surface frosting of the heat exchanger reducing significantly the thermal performance of these composite systems. In tab. 3, the No. 1 is the integrated system combining with PLHP and HP proposed in this study. The No. 2 is a hybrid system with a combination of HP and fixed-plate (sensible heat exchanger). The No. 3 is dual-loop HP heat recovery system. The No. 4 is a hybrid system composed of HP and energy wheel. The No. 5 is a traditional HP heat recovery system. As shown in the tab. 3, in summer conditions, the EER of the systems 2-5 are 2.17, 4.2, 3.3, and 2.5, respectively. In winter conditions, the EER of the system 3 and 5 are 6.9 and 6.5, respectively. Results indicate that these systems are at a low level.

Table 3. Performance comparison of the similar systems

No.	1	2	3	4	5
Reference	This study	[29]	[30]	[31]	[32]
Conditions	Winter/summer	Summer	Winter/summer	Summer	Winter/summer
Type	HP + PLHP	Plate + HP	Dual-loop HP	HP + Energy wheel	HP
T_{e1} [ºC]	20/27	27.7	20/27	27	20/27
H_{e1} [%]	40/50	50	40/50	50	40/50
T_{f1} [ºC]	−15/40	35.2	−15/40	38	−15/40
EER	11.7/5.8	2.17	6.9/4.2	3.3	6.5/2.5

Conclusions

In this paper, the mathematical model of HP heat recovery system and HP composite pump-driven loop heat pipe heat recovery system are established, the working characteristics of HP and HPCP with R32 under different indoor and OT differences are compared and analyzed. The conclusions could be drawn as follows.

- The heating capacity of the HPCP system is in line with the heating load in winter.
- The EER of HPCP is higher than that of HP under the whole year conditions. When OT is – 15 ℃, the heating EER of HPCP is 50% higher than that of HP. When OT is 40 ℃, the cooling EER of HPCP is 35% higher than that of HP. The HPCP system provides a new direction for energy-saving of heat recovery system.
- The temperature effectiveness of HPCP is higher than that of standard value, and the HPCP has a smaller deviation degree than the HP. In winter conditions, the deviation degree of HPCP and HP is 3.3 and 5.1, respectively. In summer conditions, the deviation degree of HPCP and HP is 3.4 and 5.8, respectively.
- Compared with the similar systems, HPCP has shown excellent thermal performance, which indicates that HP can be replaced by HPCP system in building ventilation.

Acknowledgment

4312

Liu, S., *et al.*: Simulation Research on Heat Recovery System of …
THERMAL SCIENCE: Year 2022, Vol. 26, No. 5B, pp. 4301-4313

Nomenclature

A — target value
Bo — boiling feature number
c_p — specific heat capacity, [$\mathrm{Jkg^{-1}K^{-1}}$]
D — outer tube diameter, [mm]
d — diameter, [mm]
De — deviation degree
Fr — Froude number
f — friction coefficient
G — mass flow, [$\mathrm{kgm^{-2}s^{-1}}$]
g — acceleration of gravity, [$\mathrm{m^2s^{-1}}$]
h — enthalpy, [$\mathrm{kJkg^{-1}}$]
L — tube length, [mm]
$\dot{m}$ — mass-flow rate, [$\mathrm{kgs^{-1}}$]
Nu — Nusselt number
n — number of tubes
P — input power, [kW]
Pr — Prandtl number
p — condensation pressure, [Pa]
p_c — critical pressure, [Pa]
Q — heat transfer capacity, [kW]
q_r — latent heat of refrigerant, [$\mathrm{kJkg^{-1}}$]
Re — Reynolds number
s — tube space
t — temperature, [ºC]
X — actual value
X_{tt} — Lockhart-Martinelli number
x — dryness fraction

Greek symbols

α — heat transfer coefficient, [$\mathrm{Wm^{-2}K^{-1}}$]
δ — fin thickness, [mm]
η — efficiency

λ — thermal conductivity, [$\mathrm{Wm^{-1}K^{-1}}$]
μ — viscosity, [Pa·s]
ξ — dehumidification coefficient
ρ — density, [$\mathrm{kgm^{-3}}$]
σ — surface tension, [$\mathrm{Nm^{-1}}$]

Subscripts

a — air
b — saturated air
c — compressor
f — fin
fan — fan
i — inter
o — outer
p — pump
g — gas
l — liquid
tp — two-phase
sat — excess
11 — exhaust air inlet
21 — fresh air inlet
22 — fresh air outlet

Acronyms

EER — energy efficiency ratio
HP — heat pump
HPCP — heat pump composite pump-driven loop heat pipe
OT — outdoor temperature
PLHP — pump-driven loop heat pipe
SBS — sick building syndrome

References

[1] Vuckovic, G. D., *et al.*, Air-Source Heat Pump Performance Comparison in Different Real Operational Conditions Based on Advanced Exergy and Exergoeconomic Approach, *Thermal science, 25* (2021), 3A, pp. 1849-1866
[2] Harminder Kaur, G. A., World Business Council for Sustainable Development, *World Environment, 4* (2012), pp. 2735-2738
[3] None, N., Building Technologies Program: Planned Program Activities for 2008-2012, Technical report, Osti.gov, US Department of Energy, Washington D.C., USA, 2008
[4] Sun, Y. X., *et al.*, Indoor Air Quality, Ventilation and Their Associations with Sick Building Syndrome in Chinese Homes, *Energy and Buildings, 197* (2019), Aug., pp. 112-119
[5] Sun, C. J., *et al.*, Outdoor Air Pollution in Relation to Sick Building Syndrome (SBS) Symptoms Among Residents in Shanghai, China, *Energy and Buildings, 174* (2018), Sept., pp. 68-76
[6] Gladyszewska-Fiedoruk, K, Krawczyk, A. K., The Possibilities Of energy consumption reduction and a Maintenance of Indoor Air Quality in Doctor's Offices Located in North-Eastern Poland, *Energy and Buildings, 85* (2014), Dec., pp. 235-245
[7] Zhang, L. Z., Niu, J. L., Energy Requirements for Conditioning Fresh Air and the Long Term Savings with a Membrane-Based Energy Recovery Ventilator in Hong Kong, *Energy, 26* (2001), 2, pp. 119-135
[8] Li, Z., *et al.*, New Type of Fresh Air Processor with Liquid Desiccant Total Heat Recovery, *Energy and Buildings, 37* (2005), 6, pp. 587-593
[9] Yamaguchi, S., Saito, K., Numerical and Experimental Performance Analysis of Rotary Desiccant Wheels, *International Journal of Heat and Mass Transfer, 60* (2013), May, pp. 51-60

[10] Hughes, B. R., *et al*., Passive Energy Recovery from Natural Ventilation Air Streams, *Applied Energy, 113* (2014),Jan., pp. 127-140

[11] Bo., Li., *et al*., Performance of a Heat Recovery Ventilator Coupled with an Air-to-Air Heat Pump for Residential Suites in Canadian Cities, *Journal of Building Engineering, 21* (2019), Jan., pp. 343-354

[12] Fernandez-Seara., J, *et al*., Experimental Analysis of an Air-to-Air Heat Recovery Unit for Balanced Ventilation Systems in Residential Buildings, *Energy Conversion and Management, 52* (2011), 1, pp. 635-640

[13] Vali, A., *et al*., Numerical Model and Effectiveness Correlations for a Run-Around Heat Recovery System with Combined Counter and Cross Flow Exchangers, *International Journal of Heat and Mass Transfer, 52* (2009), 25-26, pp. 5827-5840

[14] El-Baky, M. A. A., Mohamed, M. M., Heat Pipe Heat Exchanger for Heat Recovery in Air Conditioning, *Applied Thermal Engineering, 27* (2007), 4, pp. 795-801

[15] Wang, L., *et al*., Experimental Investigations on a Heat Pump System for Ventilation Heat Recovery of a Novel Dual-Cylinder Rotary Compressor, *Int. Journal of Refrigeration, 108* (2019), Dec., pp. 26-36

[16] Ma, G. Y., *et al*., Operating Characteristics of a Pump-Driven Loop Heat Pipe Energy Recovery Device (in Chinese), *Journal of Beijing University of Technology, 42* (2016), 7, pp. 1095-1101

[17] Zhu, C. Y., Ding, S. P., A Multistage Dynamic Heat Pipe System (in Chinese), CN 102788524A. 2012-11-21, 2012

[18] Zhou, F., *et al*., Thermal Performance of a Multi-Loop Pump-Driven Heat Pipe as an Energy Recovery Ventilator for Buildings, *Applied Thermal Engineering, 138* (2018), June, pp. 648-656

[19] Ma, A. N., *et al*., Thermodynamic Performance Analysis of a Triple-Loop Air-Source Heat Pump Heat Recovery System (in Chinese), *Journal of Refrigeration, 40* (2019), 04, pp. 17-22

[20] Wang, L., Research on Working Characteristic of Multi-Loop Heat Pump Ventilation Heat Recovery System (in Chinese), Ph. D. thesis, Beijing University of Technology, Beijing, 2020

[21] Cao, X., *et al*., Stepped Pressure Cycle -A New Approach to Lorenz Cycle, *International Journal of Refrigeration, 74* (2016), Oct., pp. 283-294

[22] Jia, X. Y., *et al*., Experimental Investigation of Parallel-Loop Heat Pump for Ventilation Heat Recovery (in Chinese), *Journal of Central South University (Science and Technology), 52* (2021), 06, pp. 1876-1882

[23] Chandrasekaran, S. K., Srinivasan, K., Experimental Studies on Heat Transfer Characteristics of SS304 Screen Mesh Wick Heat Pipe, *Thermal science, 21* (2017), Suppl. 2, pp. S497-S502

[24] Zhou, F., *et al*., Thermal Performance of a Pump-Driven Loop Heat Pipe as an Air-to-Air Energy Recovery Device, *Energy and Buildings, 151* (2017), Sept., pp. 206-216

[25] Dorao, C. A., Fernandino, M., Simple and General Correlation for Heat Transfer During Flow Condensation Inside Plain Pipes, *Int. J. of Heat and Mass Transfer, 122* (2018), July, pp. 290-305

[26] Tang, W., Li, W., Frictional Pressure Drop During Flow Boiling in Micro-Fin Tubes: A New General Correlation, *International Journal of Heat and Mass Transfer, 159* (2020), 5, 120049

[27] Zhang, J., *et al*., General Heat Transfer Correlations for Flow Boiling of Zeotropic Mixtures in Horizontal Plain Tubes, *Applied Thermal Engineering, 150* (2019), Mar., pp. 824-839

[28] ***, General Administration of Quality Supervision, Inspection and Quarantine of the People's Republic of China (in Chinese), Room air conditioners (GB/T7725-2016), Standards Press of China, 2016

[29] Li, W. Y., *et al*., Experimental Study of a Novel Household Exhaust Air Heat Pump Enhanced by Indirect Evaporative Cooling, *Energy and Buildings, 236* (2021), 110808

[30] Jia, X. Y., *et al*., Experimental Study and Operation Optimization of a Parallel-Loop Heat Pump for Exhaust Air Recovery in Residential Buildings, *Journal of Building Engineering, 45* (2022), 103468

[31] Sheng, Y., *et al*., Simulation and Energy Saving Analysis of High Temperature Heat Pump Coupling to Desiccant Wheel Air Conditioning System, *Energy, 83* (2015), Apr., pp. 583-596

[32] Ma, A. N., *et al*., Thermodynamic Performance Analysis of a Triple-Loop Air-Source Heat Pump Heat Recovery System (in Chinese), *Journal of Refrigeration, 40* (2019), 04, pp. 17-22